

Precursors and Outbursts of A 0535+26 in 2009-2011 observed by the MAXI/GSC and the Swift/BAT

Motoki NAKAJIMA,¹ Tatehiro MIHARA,² Mutsumi SUGIZAKI,² Motoko SERINO,² Masaru
MATSUOKA,²

Nobuyuki KAWAI,³ Kazuo MAKISHIMA,^{2,4,5}

¹*School of Dentistry at Matsudo, Nihon University, 2-870-1, Sakaecho-nishi, Matsudo, Chiba, JAPAN
271-8587*

²*MAXI team, RIKEN, 2-1 Hirosawa, Wako, Saitama, JAPAN 351-0198*

³*Department of Physics, Tokyo Institute of Technology, 2-12-1 Ookayama, Meguro-ku, Tokyo, JAPAN
152-8551*

⁴*Department of Physics, University of Tokyo, 7-3-1 Hongo, Bunkyo-ku, Tokyo, JAPAN 113-0033*

⁵*Research Center for the Early Universe, University of Tokyo, 7-3-1 Hongo, Bunkyo-ku, Tokyo, JAPAN
113-0033*

(MN) nakajima.motoki@nihon-u.ac.jp

(Received ; accepted)

Abstract

Over the 3-year active period from 2008 September to 2011 November, the outburst behavior of the Be/X-ray binary A 0535+26 was continuously monitored with the MAXI/GSC and the Swift/BAT. The source exhibited nine outbursts, every binary revolution of 111.1 days, of which two are categorized into the giant (type-II) outbursts. The recurrence period of these outbursts is found to be ~ 115 days, significantly longer than the orbital period of 111.1 days. With the MAXI/GSC, a low-level active period, or a “precursor”, was detected prior to at least four giant outbursts. The precursor recurrence period agrees with that of the giant outbursts. The period difference of the giant outbursts from the orbital period is possibly related with some structures in the circumstellar disc formed around the Be companion. Two scenarios, one based on a one-armed disc structure and the other a Be-disc precession, are discussed.

Key words: X-ray: stars

1. Introduction

Be/X-ray binaries are a group of high-mass X-ray binaries that consist of a neutron star and an OB-type star with Balmer emission lines (Be star). They are major members of recurrent X-ray

transients and are usually detected when they exhibit bright X-ray outbursts lasting for a week to months. During the outbursts, the X-ray luminosities increase by 3–5 orders of magnitude from those in the quiescent states. Although the mechanism of these outbursts has not been fully understood, it is considered to be related with mass accretion from the circumstellar disc of the Be star onto the neutron star.

X-ray outbursts of Be/X-ray binaries are classified into two types, normal outbursts (type-I) and giant ones (type-II) (e.g. Reig 2011). The former usually occur when the neutron star passes through the periastron, and hence repeat by the orbital period. Their peak luminosities distribute in a narrow range of $10^{36} - 10^{37}$ erg s⁻¹. Some of those sources showed moderate spin-up of the neutron star during the normal outbursts (e.g. GS 1843–02; Finger et al. 1999). On the other hand, the latter, namely giant outbursts, are characterised by their higher X-ray luminosity (typically $\geq 10^{37}$ erg s⁻¹), longer duration, less frequent occurrence, and their orbital phases out of the periastron (Priedhorsky & Terrell. 1983; Reig 2011). Since large spin-up episodes of the neutron star often accompany giant outbursts, an accretion disc is considered to form around the neutron star in occasions (Reig 2011). In addition to the observational outburst classification, a new scenario based on the analytical/numerical studies (Okazaki et al. 2013) is proposed to explain the two type of outbursts by different mass accretion mechanism.

A 0535+26 is one of the representative Be/X-ray binaries in our Galaxy. The source was discovered by the Ariel-5 satellite (Rosenberg et al. 1975; Coe et al. 1975) when it exhibited a giant outburst in 1975. The subsequent observations revealed its 103-s coherent X-ray pulsation (Rosenberg et al. 1975). The optical counterpart is the O9.7 IIIe star HD245770 at a distance of 1.8 ± 0.6 kpc (Giangrande et al. 1980). Steele et al. (1998) revised the spectral type of its optical counterpart with B0 IIIe. Its orbital elements, including the orbital period (111.1 ± 0.1 day), eccentricity (0.47 ± 0.02) and the epoch of the periastron passage (MJD=53613.0), were determined by Finger et al. (2006). Both normal and giant outbursts have been observed so far (Motch et al. 1991). The giant outbursts were observed nine times, typically every a few years (Camero-Arranz et al. 2012 and references therein). All these events occurred after the periastron passages, and were followed by a sequence of normal outbursts.

In 2008 September, the *RXTE*/ASM detected a renewed activity of A 0535+26, since the previous active period which ended in 2005 (Levine & Remillard. 2008). The new active period continued three years until 2011 November, and the source meanwhile exhibited nine outbursts including both the normal and the giant ones. This is the longest active period that has ever been observed since its discovery (Finger et al. 1996; Camero-Arranz et al. 2012).

In this paper, we report on the X-ray outbursts of A 0535+26 during the above active period, based on continuous monitoring by the MAXI/GSC (Matsuoka et al. 2009) and the Swift/BAT (Gehrels et al. 2004). The GSC onboard MAXI successfully detected not only normal / giant outbursts but also low-intensity activity during the outburst intermission (Sugizaki et al. 2009).

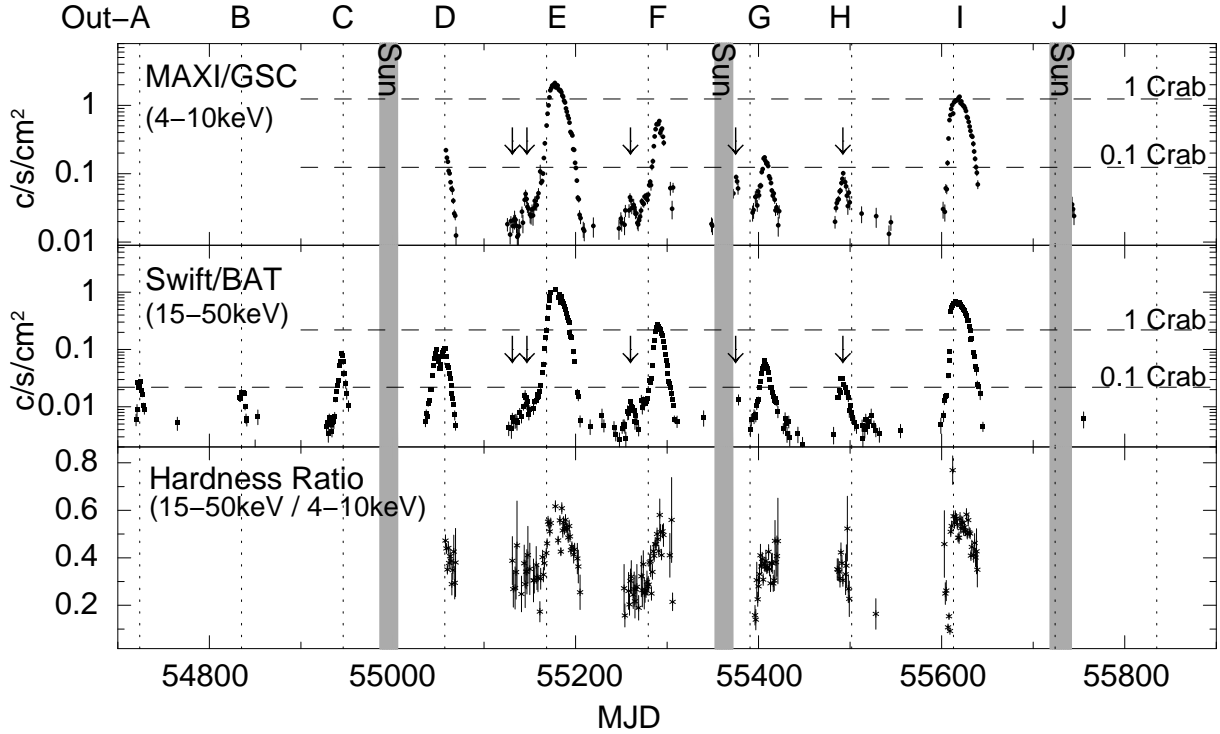


Fig. 1. Light curves of A 0535+26 from 2008 September to 2011 November, in the 4–10 keV band by the MAXI/GSC (top : 1 Crab = $1.24 \text{ c cm}^{-2} \text{ s}^{-1}$) and in the 15–50 keV band by the Swift/BAT (Middle : 1 Crab = $0.22 \text{ c cm}^{-2} \text{ s}^{-1}$). The horizontal dashed lines indicate the flux level in Crab units. The bottom panel shows hardness ratio of the Swift/BAT to the MAXI/GSC. The vertical dotted lines, the arrows, and the gray belts represent the periastron passages (Finger et al. 2006), precursors, and periods of the Sun avoidance of the MAXI/GSC, respectively.

2. Observations

2.1. MAXI/GSC

Since the in-orbit operation started in 2009 August, the Gas Slit Camera (GSC) (Mihara et al. 2011; Sugizaki et al. 2011) onboard MAXI on the International Space Station scans almost the entire sky in every ISS orbital period of about 92 minutes. For ~ 45 s typically every 92 minutes, the GSC observes an X-ray source in any position on the sky, except an area which is within $\lesssim 10^\circ$ of the Sun. In the web page¹, the MAXI team provides GSC light curves of about 300 cataloged X-ray sources including A 0535+26, for three energy bands of 2–4, 4–10 and 10–20 keV. Since the data in the 4–10 keV band have the highest signal-to-noise ratio, we hereafter use this energy band to extract the MAXI/GSC light curves.

¹ <http://maxi.riken.jp/top/>

2.2. *Swift/BAT*

The Swift Burst Alert Telescope (BAT; Barthelmy et al. 2005) has performed all-sky hard X-ray survey in the 15–50 keV energy band since the operation started in 2004. The Swift/BAT team provides light curves for about a thousand of cataloged X/gamma-ray sources via the archive web page². We obtained the light curve data of A 0535+26, and utilized good-quality data selected with a quality flag = 0.

3. Analysis and Results

3.1. *Long-term Light Curve and Hardness Ratio*

Figure 1 shows the X-ray light curves of A 0535+26 observed with the MAXI/GSC (2009 August 15 to 2011 November 30) and the Swift/BAT (2008 September 1 to 2011 November 30), over those periods when significant flux was detected above 3σ of the statistical uncertainty. The hardness ratio of the Swift/BAT band to the MAXI/GSC band is shown in the bottom panel. Nine sequential outbursts are clearly recognized in the Swift/BAT light curve with 111.1-days orbital cycle. As shown in figure 1, we hereafter call them Out-A, B, C, ..., and J.

The first three outbursts, namely Out-A, B, and C, exhibited their peaks at times approximately consistent with periastron passages. The peak intensity of Out-A and Out-B are all ~ 0.1 Crab in the 15–50 keV band, while that of Out-C is about 4 times higher, ~ 0.4 Crab. The outburst profile changed clearly after Out-D: the profiles of Out-A, B, and C are single-peaked, whereas Out-D has a double-peaked profile (Caballero et al. 2011; Caballero et al. 2013).

After Out-D, MAXI started the operation in orbit, and as indicated by arrows in figure 1, the GSC started detecting even periods of weaker X-ray emission at an earlier orbital phase than the periastron (Sugizaki et al. 2009). They are more easily recognized in the zoomed light curves in figure 2. We call this type of event a “precursor”. These precursors were also detected with the BAT (figure 1 middle). In particular, those preceding Out-E are found to involve little changes in the hardness ratio (figure 1 bottom).

The subsequent outburst, Out-E, developed into a giant one, and the peak 4–10 keV intensity reached ~ 1.8 Crab. The source reached the outburst maximum 9.3 d after the periastron, and the hardness ratio changed significantly across the outburst. Assuming that the X-ray emission is isotropic and the spectrum shape is like the Crab nebula, the total X-ray energy released during the outburst period (MJD=55157–55201) in the 4–10 keV band is estimated to be 1.1×10^{43} erg from the daily MAXI/GSC light curve.

The next outburst, Out-F, also developed into a large one, and the peak phase was further delayed. A precursor was also seen ~ 30 days before Out-F. The next precursor preceding Out-G was observed by the MAXI/GSC but not by the Swift/BAT due to the Sun angle limit. Fermi/GBM pulsar monitor detected an increase of pulsed flux both in the precursor and the mainbody of Out-G

² <http://swift.gsfc.nasa.gov/docs/swift/results/transients/>

(Camero-Arranz et al. 2012). The peak of Out-G was also delayed from the periastron. The hardness ratio also increased similarly as the outburst developed. However, it did not reach the level of the peak of Out-E. The change of the peak intensity apparently has a positive correlation with the peak hardness in these outbursts.

In Out-H, the intensity reached a maximum before the periastron. No activity was seen before the peak in the MAXI/GSC or the Swift/BAT data. Instead, a possible post-outburst activity is seen in the Swift/BAT data on MJD \sim 55523, or at on orbital phase of ~ 0.2 .

After the relatively weak Out-H, we observed yet another giant outburst, Out-I, which exhibited the peak 4-10 keV intensity of ~ 1 Crab. No precursor was seen in either the MAXI/GSC or the Swift/BAT data. The hardness ratio changed with the flux similarly as in Out-E.

The next periastron after Out-I was observable with neither mission due to the Sun avoidance. However, the positive flux detected on MJD \sim 55745 suggests the presence of another outburst (Out-J). This possibly faint outburst was not observed by the Fermi/GBM. After that, no significant flux have been observed from the source till the end of 2012.

In addition to the X-ray activities, significant optical variations have also been reported in these period (Moritani et al. 2011; Camero-Arranz et al. 2012; Yan et al. 2012). The V-band magnitude started to decrease in the epoch of Out-A and then reach the quiescent level in the Out-D. On the other hand, the equivalent width of H α line increased around the Out-D and then decreased after the Out-F.

3.2. *Evolution of Outburst Orbital Phase*

As described in the previous section, the outbursts (Out-E, F and G) and the precursors both exhibited significant offsets in orbital phase from the periastron passages. In this paper, we calculated the epoch of periastron passages using the orbital elements in Finger et al. (2006), which were determined from X-ray observations in 2005. Judging from the precision of the orbital period (111.1 ± 0.1 d), the error of the extrapolated periastron time in 2009–2011 is ~ 1 d at most. In order to better visualize this effect, figure 2 shows the same light curves, but in cycle-by-cycle form, against the orbital phase. Thus, we find a clear systematic shift, from Out-E to Out-G, in the orbital phase of the outburst peak. The precursor phase (marked by arrows in figure 2) also shifted similarly to the main peak. Among these outbursts, the intervals between the precursor and the outburst are almost constant at ~ 30 days (or ~ 0.27 orbital phase).

Interestingly, Out-H, which did not develop into a large one, consisted of two peaks like Out-D. The former event can be identified as a precursor based on an orbital-phase extrapolation from Out-E, F, and G. The second peak can be considered as a main outburst, although its intensity is smaller than that of typical outburst. In the next outburst, Out-I, the peak just came after the periastron, and neither a precursor nor a post-outburst flare were observed.

To be quantitative, we fitted individual outburst / precursor profiles with a Gaussian function and determined their peak phases. Since some outbursts exhibit asymmetric profiles which cannot be

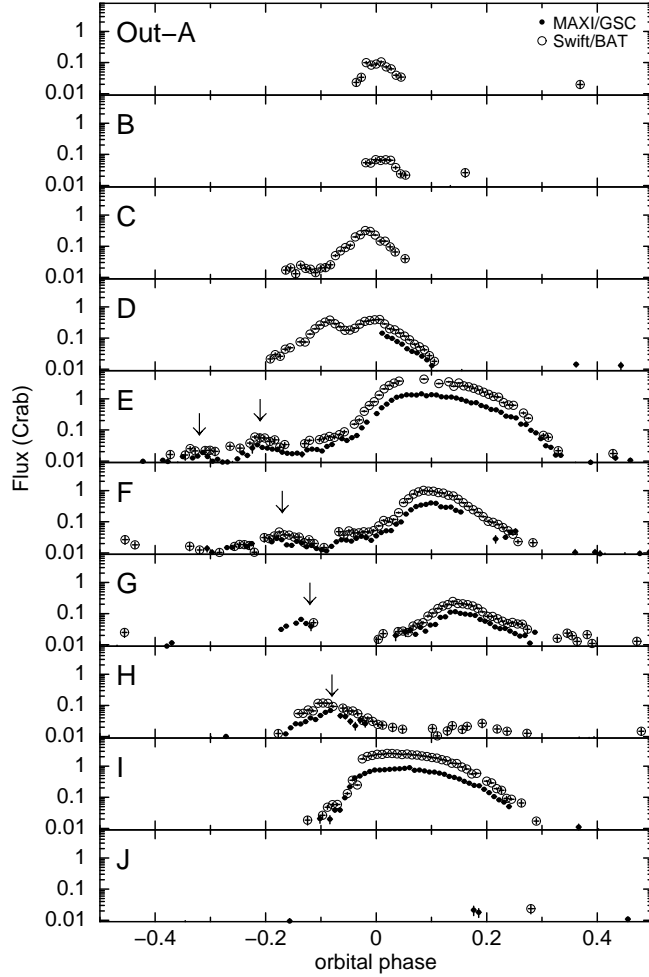


Fig. 2. The same light curves as in figure 1, but shown for individual 111.1-d orbital cycles and those fluxes in Crab units. The MAXI/GSC(4–10 keV) and the Swift/BAT(15–50 keV) data are plotted in the same panel with different marks. The flux conversion factors between the count rates and Crab units are same as in figure 1. The origin of the orbital phase (= 0) corresponds to the periastron passage. Five arrows in panels E, F, G, and H indicate precursor peaks.

reproduced by a single Gaussian function, we performed the fit within a narrow range around the peak such that the fit is accepted reasonably. In addition, we confirmed that the result does not depend on the chosen fitting range.

The above analysis has given the best-fit epochs as tabulated in table 1, and plotted in figure 3. The peak phases of Out-A, B, C and the second peak of Out-D agree with the expected periastron passage within the precision of 1 d (= 0.009 in orbital phase). The first peak of Out-D emerged ~ 0.1 orbital phase before the periastron passage. After the anomalous Out-D, the four outbursts (Out-E, F, G and H) show a systematic drift in the phases of the emission peak and of the precursor, indicating that their recurrent period is longer than the orbital period. To evaluate the rates of the phase shifts, we fitted the large-outburst and precursor data points in figure 3 with a linear function, and show the results by a solid and a dashed lines. The phase-shift rates of the outbursts and the precursors were

Table 1. Dates and orbital phases of outbursts and precursors

		MAXI		Swift	
		MJD	orbital phase ^a	MJD	orbital phase ^a
outburst	A	—	—	54,724.5 ± 0.2	0.0045 ± 0.0009
	B	—	—	54,835.9 ± 0.5	0.0072 ± 0.0045
	C	—	—	54,944.5 ± 0.1	0.9847 ± 0.0009
	D	—	—	55,047.1 ± 0.1	0.9082 ± 0.0009
	D ^b	—	—	55,056.9 ± 0.1	0.9964 ± 0.0009
	E	55,177.7 ± 0.2	0.0837 ± 0.0018	55,178.4 ± 0.2	0.0900 ± 0.0018
	F	55,291.1 ± 0.1	0.1044 ± 0.0009	55,289.7 ± 0.3	0.0918 ± 0.0027
	G	55,407.3 ± 0.1	0.1503 ± 0.0009	55,407.4 ± 0.2	0.1512 ± 0.0018
	H	—	—	55,521.9 ± 3.0	0.1818 ± 0.0270
precursor	I	55,617.9 ± 0.1	0.0459 ± 0.0009	55,617.4 ± 0.2	0.0414 ± 0.0018
	E	55,132.4 ± 1.9	0.6760 ± 0.0171	55,132.9 ± 0.7	0.6805 ± 0.0063
	E ^c	55,146.2 ± 0.8	0.8002 ± 0.0072	55,145.7 ± 0.7	0.7957 ± 0.0063
	F	55,259.8 ± 0.5	0.8227 ± 0.0045	55,261.2 ± 0.7	0.8353 ± 0.0063
	G	55,378.4 ± 1.1	0.8902 ± 0.0099	—	—
	H	55,492.5 ± 0.3	0.9172 ± 0.0027	55,492.5 ± 0.2	0.9172 ± 0.0018

^a:Orbital elements in Finger et al. (2006) are employed.

^b:Second peak of the outburst D on MJD 55050.

^c:Second precursor of the outburst E on MJD 55180.

obtained as $(3.03 \pm 0.06) \times 10^{-4}$ phase day⁻¹ and $(3.62 \pm 0.12) \times 10^{-4}$ phase day⁻¹, respectively, with the errors of 1- σ confidence limit. The phase shift of the precursor is slightly faster than that of the main outburst.

Next, we evaluate recurrent periods of the outbursts and the precursors, P_{out} and P_{pre} , respectively. Using the obtained phase-shift rate s in unit of day day⁻¹, P_{out} and P_{pre} are related to the orbital period, P_{orb} , as

$$P_{\text{out,pre}} = \frac{P_{\text{orb}}}{1 - s}. \quad (1)$$

The outburst and precursor periods calculated in this way are 115.0 ± 0.1 day and 115.8 ± 0.2 day, respectively. Figure 4 shows the light curves folded by the derived outburst beat period (115.0 day), where the outburst and precursor peaks are both observed to align well.

3.3. Evolution of Outburst Peak-Intensity

As seen in the light curves of figure 1, the four outbursts (Out-E to H) changed not only in their orbital phase, but also in their intensity. As shown in figure 5, their peak fluxes decreased exponentially, with an e-folding time of 90.8 ± 1.3 days estimated with the MAXI/GSC data and

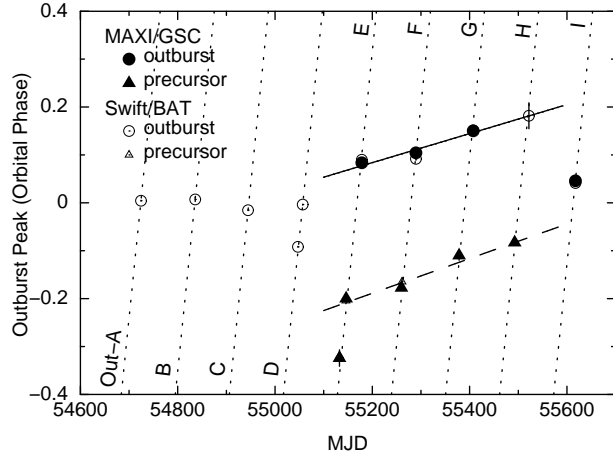


Fig. 3. Orbital phases of the outburst peaks (circles) and precursors (triangles) taken from table 1, plotted as a function of MJD. Filled symbols are those obtained from the MAXI/GSC (4–10 keV) data, and open ones are from the Swift/BAT (15–50 keV) data. Solid and dashed lines indicate the best-fit linear function for the peaks and precursors of Out-E to Out-H, respectively. Dotted lines represent the orbital motion of the neutron star.

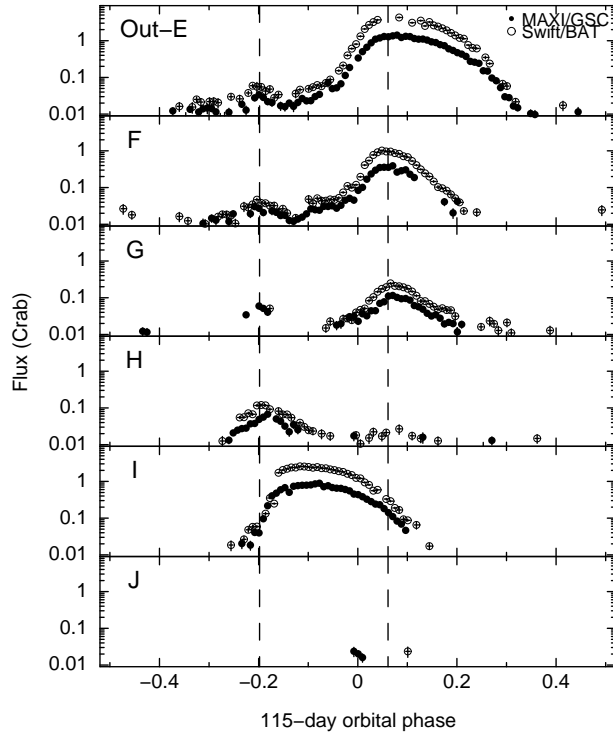


Fig. 4. Same as figure 2, but the light curves are folded by the best-fit recurrent period of 115 days of the four outburst peak from E to H. Two vertical dashed lines indicate the peak positions of the precursors and outbursts in Out-E to H. The 115day phase 0 is taken at the true orbital phase 0 of Out-E.

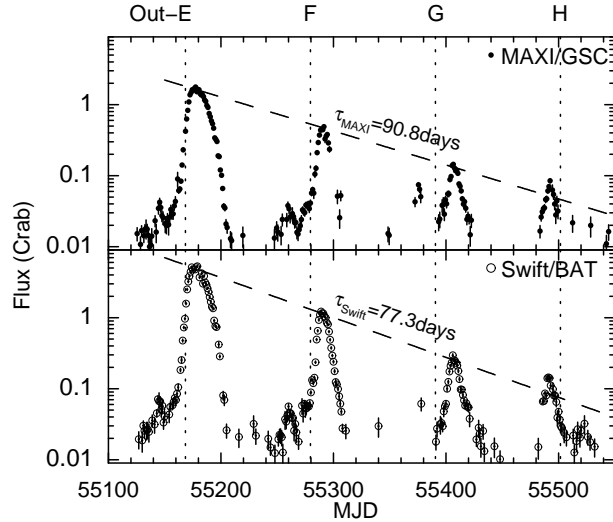


Fig. 5. The expansion of the four outbursts. The dotted lines represent the periastron passage. The peak intensities of the three outbursts decays exponentially (see text).

77.3 ± 1.4 days with that of Swift/BAT. Here again the errors are in $1-\sigma$.

After the outburst peak intensities thus decayed exponentially till Out-H, the next one, Out-I, violated this systematic behavior, and actually developed into the second largest one. The next expected outburst was during the Sun avoidance. Nevertheless, we can estimate that the decay time scale should be < 57 days, considering the lack of significant signals at two orbital periods later (MJD \simeq 55830).

The precursor peak intensities exhibited no systematic changes. Specifically, the precursors of Out-E and Out-F have almost the same intensity of ~ 50 mCrab (4-10 keV), that of Out-G is not clear but is probably ~ 80 mCrab, and that of Out-H is 100 mCrab.

4. Discussion

We analyzed long-term X-ray light curves of A 0535+26 obtained by the MAXI/GSC (4–10 keV) and the Swift/BAT (15–50 keV) during the active season from 2008 September to 2011 November. This is the longest active period of this X-ray source that has ever been observed since its discovery in 1975. The source exhibited nine outbursts which are approximately synchronized with the binary period of 111.1 d. Four of them recurred every 115 d which is significantly longer than the binary period. In both data sets, we also found low-level active periods, or precursors, which preceded the large outbursts. Below, we discuss the cause of the asynchronous outburst occurrence and of the precursor activity.

4.1. Classification of Outbursts – Normal (Type-I) or Giant (Type-II)

Outbursts in Be/X-ray binaries are classified into normal (type-I) and giant (type-II) ones, according to their luminosity and orbital phase at the flux peak (e.g. review by Reig 2011). Normal

outbursts have peak luminosities below $\sim 10^{37}$ erg s $^{-1}$, and occurs at or near the periastron passage of the neutron star. Giant outbursts exhibit higher luminosities exceeding $\sim 10^{37}$ erg s $^{-1}$, and their orbital phases do not necessarily coincide with the periastron. According to the classical definition, we can classify Out-A, B, and C into normal, while Out-E and I readily into giant ones. On the other hand, the other outbursts, Out-D, F, G and H, cannot be categorized into either type. As pointed out by Kretschmar et al. (2013), the simple classification cannot be always applied. From the monotonical peak-phase shift (figure 2 and figure 3) and exponential decay of the peak fluxes (figure 5), we presume that the giant outburst (Out-E) and the following ones (Out-F, G, and H) have the same mechanism. Those followings might be named as "giant outburst remnant".

In addition to the variety in the luminosity and the orbital phase as described above, Out-D, has a peculiar double-peaked profile. So far, outbursts with such a double-peaked profile have been observed three times from this source, in 1993 (July and November ; Finger et al. 1996) and 2005 August (Caballero et al. 2008; Postnov et al. 2008; Caballero et al. 2011; Caballero et al. 2013). However, the latter event is a "pre-outburst flare" which lasted for less than a few hours (Postnov et al. 2008; Caballero et al. 2011); we consider it as a different phenomenon from the double-peaked outburst such as Out-D, whose duration (~ 10 days) is much longer. In addition to A 0535+26, such double-peaked outbursts have been observed from two other Be/X-ray binaries, XTE J1946+274 (Müller et al. 2012) and GX304-1 (Nakajima et al. 2012). Among those three sources, A 0535+26 and GX304-1 exhibited giant outbursts after the detection of a double-peaked outburst. Therefore, double-peaked outbursts might be considered as a sign of the recurrence of giant outbursts (Nakajima et al. 2012; Caballero et al. 2013), and may be recognized as an intermediate class between the normal and giant ones.

4.2. Phase Shift and Intensity Evolution of Giant Outbursts

As analyzed in section 3, the outburst-peak phase shifted steadily through the four giant outbursts, from Out-E to Out-H, and their peak intensity decayed on a time scale of 77–91 d. Such an effect has been observed from two other Be/X-ray binaries : EXO 2030+375 (Wilson et al. 2002) and GS 0834-430 (Wilson et al. 1997). However, the precursor phase shift observed in the present study was not reported from the other sources. Furthermore, the phase shift in A 0535+26 (~ 20 days) is much larger than that of EXO 2030+375 (~ 5 days).

Since X-ray intensity is considered to provide a probe of the circumstellar disc of the Be star along the neutron-star orbit, the outburst phase shift is considered to reflect density profiles in the Be disc. Let us assume that dense parts are produced in the disc by some perturbations, and that they rotates with a certain rotational frequency, ν_{per} . We further assume that it couples with the orbital frequency $\nu_{\text{orb}} = P_{\text{orb}}^{-1} = 1/111.1 \text{ d}^{-1}$ to produce a beat frequency ν_{beat} as,

$$\nu_{\text{orb}} - \nu_{\text{per}} = \nu_{\text{beat}}, \quad (2)$$

and identify ν_{beat}^{-1} with the period $P_{\text{out}} = 115 \text{ d}$ with which the consecutive giant outbursts emerged. Equation (2) then yields $\nu_{\text{per}} = 3.13 \times 10^{-4} \text{ d}^{-1}$, which corresponds to a period of ~ 8.7 years. Below,

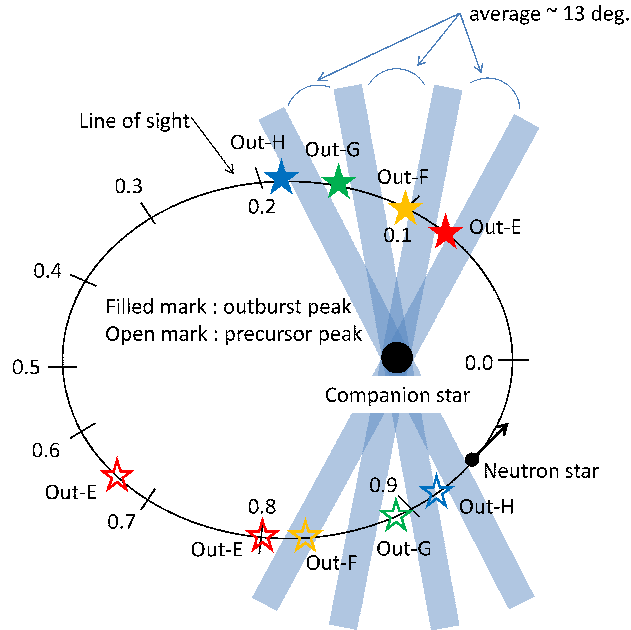


Fig. 6. Orbital geometry of A 0535+26. The open and filled symbols represent the positions of the precursor peaks and of the main outbursts respectively.

we discuss two possible scenarios to explain the orbital phase shift of the outbursts including this ν_{beat} , referring to figure 6 which summarizes the present observations.

4.3. Global One-armed Oscillation Scenario

One possible explanation of the evolution of the outburst profile is a model of density perturbation called “global one-armed oscillation” on a Be disc (e.g. Okazaki 1991; Papaloizou et al. 1992; Okazaki 1997), proposed to explain long-term variations of double-peaked (violet and red) $H\alpha$ emission lines (Silaj et al. 2010 and references therein). The violet-to-red intensity ratio, so called V/R ratio, varies on timescales of years to decades. The one-armed oscillation model explains it as due to a slow rotation of a dense part on the disc. Although various oscillation modes can be excited when the disc is formed, those with $m \neq 1$ (m being the azimuthal wave number) are supposed to dissipate sooner and finally only the one-armed ($m = 1$) oscillation will remain.

Previous optical studies on A 0535+26 (Moritani et al. 2010) reported that the source exhibited V/R variations with a ~ 500 d quasi-periodicity from MJD ~ 53700 to MJD ~ 55000 . It suggests the emergence of the one-armed oscillation mode. In that period, $H\alpha$ EW representing the density at the outer part of the Be disc and its size, began to increase gradually at around MJD ~ 54600 (Yan et al. 2012; Camero-Arranz et al. 2012). When the Be disc extended and reached the periastron of the neutron star, normal outbursts would occur. This can explain the three successive normal outbursts from Out-A to Out-C.

While the $H\alpha$ EW increased, the V-band brightness decreased (Yan et al. 2012; Camero-Arranz et al. 2012). This suggests the production of a low-density region at an inner part of the Be

disc (Yan et al. 2012), which would expand slowly outwards to produce a low-density ring structure. This can account for the double-peak outburst in Out-D (Yan et al. 2012).

After Out-D, the V/R variation did not follow the 500 d periodicity any longer (Moritani et al. 2011; Moritani et al. 2013), presumably due to some changes in the physical condition of the Be disc (Negueruela et al. 1998). In fact, the V-band brightening around MJD 55100 (Yan et al. 2012) and the very large H α EW around MJD 55150 (Yan et al. 2012; Camero-Arranz et al. 2012) suggest an episodic mass ejection from the Be-star equator. The emerged high-density region would propagate to the outer part of the disc on a time scale of one orbital cycle (Okazaki 1991; Moritani et al. 2011), and then expand the Be disc extremely. The high-density region of the perturbed disc is expected to rotate slowly around the Be star. If its period is $\sim 8.7 \text{ yr} = \nu_{\text{beat}}^{-1}$, the observed peak-phase shift of the outbursts can be explained.

Besides the outbursts, the precursors also emerged with 115 d periodicity from Out-E to Out-H. Since the precursors appeared at nearly opposite orbital locations of the giant outbursts (figure 6), they may be explained by the density perturbation in an unstable $m = 2$ oscillation mode which embeds a two-arm structure.

The estimated rotational period of the density perturbation ($\sim 8.7 \text{ yr}$) is considerably longer than the typical V/R variation period of $1 \sim 1.5 \text{ yr}$ (Clark et al. 1998; Moritani et al. 2010) and comparable to the statistical mean of the V/R variation periods of isolated Be stars, $\sim 7 \text{ yr}$ (Okazaki 1991 and references therein). Optical observations of A 0535+26 (figure 2 of Moritani et al. 2011 and figure 4 of Camero-Arranz et al. 2012) indicate that there would be a longer V/R variation period when the outburst orbital phase shift appeared. This anomalous V/R variation lasted for $\sim 1 \text{ yr}$, and vanished when a rapid variation (period of $\sim 25 \text{ d}$) arose in 2010 October (Camero-Arranz et al. 2012).

4.4. *Be-disc Precession Scenario*

Another scenario to explain the orbital phase shift of the outbursts is a Be-disc precession. The idea is proposed by Negueruela et al. (2001) to explain the behaviors of 4U 0115+63. According to this scenario, a Be disc does not grow as an equatorial planar disc any more when a large amount of gas is emitted. Instead, the disc is considered to be warped by the interaction with the neutron star, and tilted. The tilted disc starts precessing. The scenario, applied to A 0535+26, is illustrated in figure 7. Okazaki et al. (2013) and Moritani et al. (2013) also examined a similar tilted Be-disc geometry to explain the variety of observed outburst behaviors, which are largely classified into the normal or the giant one. They suggested that giant outbursts could occur if a Be disc is misaligned with a binary orbital plane and sufficiently developed so that a neutron star can capture a large amount of mass via Bondi-Hoyle-Lyttleton (BHL) accretion. We here employ the tilted Be-disc geometry to explain the observed outburst orbital-phase shifting.

Both the optical and X-ray observations suggest that a large amount of gas was ejected from the Be-star equator after Out-D as described in subsection 4.3. As a consequence, a tilted and sufficiently

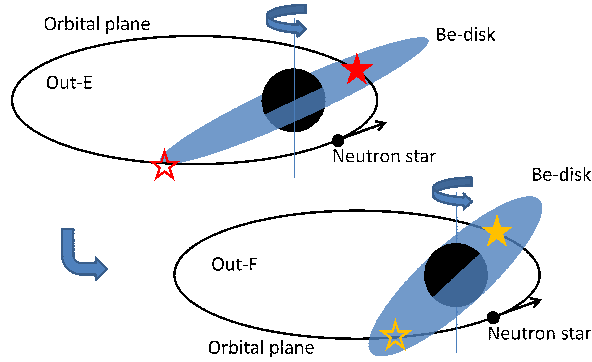


Fig. 7. Schematic illustration of the Be-disk precession scenario, in which precursors and giant outbursts occur at the moving intersections between the neutron star orbit and the Be disc.

developed disc may be formed and start a prograde precession. In fact, we can see in figure 6 that each outburst and the associated precursor occurred at nearly opposite orbital locations with respect to the Be star, and their peak locations were delayed every binary orbit by $0.02 \sim 0.04$ orbital phase. These results can be explained by such a scenario that the precursor and the main outburst occur at the two intersections between the neutron star orbit and the Be disc plane. The recurrence period of the giant outbursts, 115 d, can be explained if the disc precesses by the phase shift rate s , which is 13° per pulsar's orbital period of 111.1 d (see figure 6). We also noticed that there is a inconsistency in the Be disc precession period between our result (~ 8.7 yr) and the previous ones (674 or 886 d ; Moritani et al. 2013), although such a comparison is beyond the scope of this paper. The intensity of precursors grew up with time, since these orbital phase became closer to the periastron where the disc density is thickest. The main peak intensity declined vice verse as it became further away from the Be star with time.

In this scenario, the Out-H peak at around MJD= 55490 is considered as a precursor, and the smaller peak later at around MJD= 55520 is considered as a main outburst. Thus, the intensities of the main peaks and the precursors of Out-E, F, G, and H can be considered to represent the density change with time of the tilted Be disc formed at around Out-D. This scenario thus gives a reasonable explanation to the present observation, except the first of the two precursors of Out-E : another smaller tilted or warped disc would be required for it. Further modeling of the Be disc is left for future works.

5. Conclusion

Over the 2009 August – 2011 March active period of the Be/X-ray binary pulsar A 0535+26, nine outbursts were detected, of which two are categorized into giant (type-II) outbursts according to the peak intensity and the orbital phase. The giant outbursts and subsequent outbursts recurred with a period of 115 d, which is significantly longer than the 111.1 d orbital period. Prior to these phase-shifting outbursts, we detected the precursors, which also repeated with the 115 d period. This period shift is considered to reflect some structure, of the circumstellar disc formed around the Be

companion star. If such structures have an intrinsic period of ~ 8.7 yr, the observed giant-outburst period can be explained by its beat with the orbital period. Two possible scenarios for such a disc perturbation were discussed. One is the one-armed density perturbation on the Be disc, which is inferred from the optical spectroscopy of $H\alpha/He_I$ emission lines. The other is the precession of the Be disc, which is suggested by the orbital positions of the giant outbursts and precursors. The latter scenario reminds us a model of giant outbursts proposed by Okazaki et al. (2013) that they could occur when a misaligned Be disc is developed sufficiently. Further modeling of the Be disc is left for future works.

We appreciate all MAXI team members for their dedicated works to enable the science analysis. This research has made use of Swift/BAT transient monitor results provided by the Swift/BAT team at the Goddard Space Flight Center and Los Alamos National Laboratory. The present research work is partially supported by the Ministry of Education, Culture, Sports, Science and Technology (MEXT), Grant-in-Aid for Science Research 24340041.

References

- Barthelmy, S. D. et al. 2005, *Space Sci. Rev.*, 120, 143
Caballero, I. et al. 2008, *A&A*, 480, L17
Caballero, I. et al. 2011, *astro-ph/1107.3417*
Caballero, I. et al. 2013, *ApJ*, in print
Camero-Arranz, A. et al. 2012, *ApJ*, 754, 20
Clark, J. S. et al. 1998, *MNRAS*, 294, 165
Coe, M. J. et al. 1975, *Nature*, 256, 630
Finger, M. H. et al. 1996, *ApJ*, 459, 288
Finger, M. H. et al. 1999, *ApJ*, 517, 449
Finger, M. H. et al. 2006, in *BAAS*, Vol. 38, *BAAS*, 359
Gehrels, N. et al. 2004, *ApJ*, 611, 1005
Giangrande, A. et al. 1980, *A&AS*, 40, 289
Kretschmar, P., Nespoli, E., Reig, P., & Anders, F. 2013, *arXiv:1302.3434*
Levine, A. M. & Remillard, R. A. 2008, *ATel*, 1725
Matsuoka, M. et al. 2009, *PASJ*, 61, 999
Mihara, T. et al. 2011, *PASJ*, 63, 623
Moritani, Y. et al. 2010, *MNRAS*, 405, 467
Moritani, Y. et al. 2011, *PASJ*, 63, 25
Moritani, Y. et al. 2013, *PASJ*, in press
Motch, C. et al. 1991, *ApJ*, 369, 490
Müller, S. et al. 2012, *A&A*, 546, 125
Nakajima, M. et al. 2012, *ATel*, 4420
Negueruela, I. et al. 1998, *A&A*, 336, 251

Negueruela I. et al. 2001, A&A, 369, 117
Okazaki, A. 1991, PASJ, 43, 7
Okazaki, A. 1997, A&A, 318, 548
Okazaki, A. T., Hayasaki, K., & Moritani, Y. 2013, PASJ, 65, 41
Papaloizou, J. C., Savonije, G. J., & Henrichs, H. F. 1992, A&A, 265, L45
Porter, J., M. 1998, A&A, 336 966
Postnov, K. et al. 2008, A&A, 480, 21
Priedhorsky, W. C., Terrell, J. 1983, Nature, 303, 681
Reig, P. 2011, Astrophys. Space Science 332, 1
Rosenberg, F. D. et al. 1975, Nature, 256, 628
Silaj, J. et al. 2010, ApJ, 187, 228
Steele, I. A. et al. 1998 MNRAS, 297, L5
Sugizaki, M. et al. 2009, ATel, 2277
Sugizaki, M. et al. 2011, PASJ, 63, 635
Wilson, C. A. et al. 1997, ApJ, 479, 388
Wilson, C. A. et al. 2002, ApJ, 570, 287
Yan, J. et al. 2012, ApJ, 744, 37